

Data-adaptive unfolding of nonergodic spectra: Application to disordered ensembles

Ruben Fossion^{*1,2}

¹*Centro de Ciencias de la Complejidad (C3), Universidad Nacional Autónoma de México, 04510 México D.F., Mexico*

²*Instituto Nacional de Geriátria, Periférico Sur No. 2767, 10200 México D.F., Mexico*

The statistics of spectral fluctuations is sensitive to the unfolding procedure that separates global from local properties. Previously, we presented a parameter-free unfolding method applied to standard Gaussian ensembles of Random Matrix Theory (RMT). More general ensembles often break the ergodicity property, leading to ambiguities between spectrum-unfolded and ensemble-unfolded fluctuation statistics. Here, we use a disordered random-matrix ensemble with tunable nonergodicity to study its effect on the unfolding. We show that spectrum and ensemble averages can be calculated consistently using the same data-adaptive basis of normal modes. In this context, nonergodicity is explained as a breakdown of the common normal-mode basis.

PACS numbers: 05.45.Tp, 05.45.Mt, 89.75.-k, 02.50.Sk

I. INTRODUCTION

In standard Random Matrix Theory (RMT), the matrix elements are determined independently from a Gaussian distribution [1]. The resulting canonical Gaussian ensembles have been enormously successful in the modelling of the fluctuations of quantum excitation spectra [2], and recently they have been used as well to model the fluctuations in the eigenspectra of correlation matrices of complex systems in the classical world [3].

However, this RMT modelling is not completely realistic and there has been a search for models whose randomness would mimic physical reality closer. For example, many-body systems are effectively governed by one- and two-body forces, while canonical RMT assumes many-body forces between the constituents, so that a stochastic modelling of the one- and two-body interaction would yield a much smaller number of independent random variables than used in canonical RMT [4, 5]. Hence the interest in sparse matrices [6], band- or tridiagonal matrices [7, 8] and specialized models such as the two-body random ensemble (TBRE) [9, 10] and the more general k -body embedded Gaussian ensembles (EGE) [11]. Other generalizations determine the matrix elements from a stable but non-Gaussian distribution, in particular the Lévy distribution [12]. Also, the statistical properties of addition [13] or multiplying [14–16] of random-matrix variables has been investigated.

These new features pose the question whether a more realistic stochastic modelling of many-body systems might yield results which differ from the canonical RMT predictions. The main features of the new ensembles are correlations among matrix elements [17, 18], Gaussian instead of semicircular global eigenvalue densities [10], breaking of the power-law behaviour of the integrated level density fluctuations [6–8] and nonergodicity [5].

One of the obstacles in the statistical study of fluctuations of canonical Gaussian and more general RMT ensembles is the *unfolding* procedure which serves two purposes: (i) to separate the global level density $\bar{\rho}(E)$ from the local fluctuations $\tilde{\rho}(E) = \rho(E) - \bar{\rho}(E)$ and (ii) to rescale and normalize the fluctuations so that the statistics of different systems can be compared. The unfolding procedure is not trivial, and statistical results are sensitive to the unfolding applied, both in the quantum [19] as in the classical world [20]. If the ensemble under study is *ergodic*, then *spectrum-unfolded* and *ensemble-unfolded* fluctuation statistics are equivalent. The breaking of ergodicity creates an ambiguity in the characterization of the spectral fluctuations because both measures lead to different results (see e.g. [5]). Nevertheless, applying an appropriate unfolding to nonergodic ensembles is supposed to produce the same fluctuations pattern as observed for the canonical Gaussian Orthogonal Ensemble (GOE) from RMT [15].

In a previous publication [21], we proposed an unfolding method that is data-adaptive and parameter-free, and applied it to the canonical Gaussian ensembles of RMT. Each spectrum was decomposed exactly as the sum of normal modes that constitute a basis for the whole ensemble. The dominant modes are monotonous and describe the global spectral properties, whereas the other modes oscillate and constitute the fluctuations. An advantage of the method is that already during the unfolding procedure an ensemble estimate is obtained for the spectral rigidity in terms of the scaling behaviour of the normal modes. On the other hand, the scaling of the fluctuations of each spectrum can also be studied individually, which leads to a spectrum estimate of the ergodicity. In the case of ergodic Gaussian ensembles, both estimates are identical. In the present contribution, we consider a recently proposed disordered random-matrix model [15, 16], which allows to fine-tune the intensity of nonergodicity, to study its effect on the spectrum and ensemble estimates within the data-adaptive unfolding method.

*Email: fossion@nucleares.unam.mx

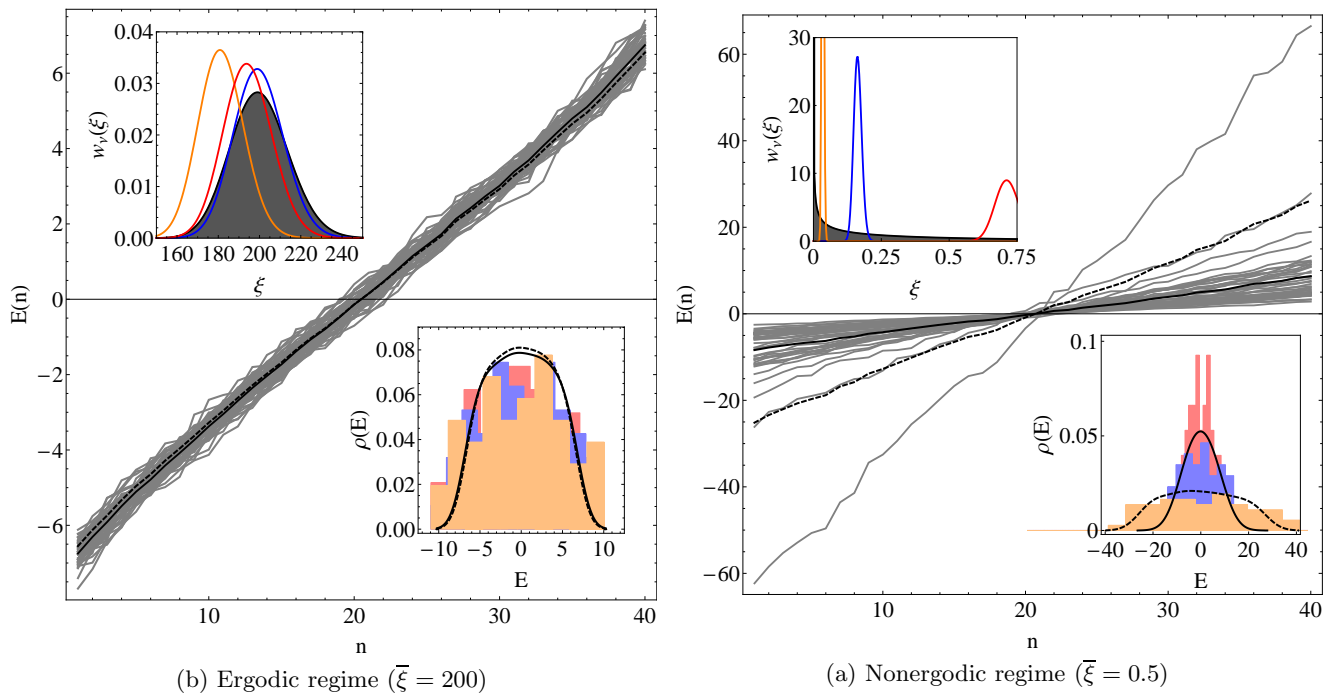


FIG. 1: Disordered ensemble with M realizations of eigenspectra with N levels, using $N = M = 50$, for different shapes of the initial disorder distribution: (a) a Gaussian-shaped gamma distribution $w_0(\xi)$ for $\bar{\xi} = 200$, and (b) a long-tailed gamma distribution $w_0(\xi)$ for $\bar{\xi} = 0.5$. (Upper left insets) Three different realizations are shown for the convergence of the disorder distribution $w_\nu(\xi)$ (non-shaded curves) towards similar positions along the initial gamma distribution $w_0(\xi)$ (black shaded curve) for $\bar{\xi} = 200$, and to very different positions for $\bar{\xi} = 0.5$. (Lower right insets) Eigenvalue density histograms $\rho(E)$ of the same three realizations, which are ergodic for $\bar{\xi} = 200$, and nonergodic for $\bar{\xi} = 0.5$. (Main figure) Eigenvalue sequences $E^{(m)}(n)$ (continuous grey lines) for all $m = 1, \dots, M$ realizations, which are ergodic for $\bar{\xi} = 200$, and nonergodic for $\bar{\xi} = 0.5$. Also shown are the parameter-free and data-adaptive global behaviour $\bar{E}(n)$ and $\rho(\bar{E})$ for one particular realization (dashed black line), and the ensemble average $\langle E(n) \rangle$ and $\langle \rho \rangle$ (continuous black lines). For the matrix dimensions $N \times N$ used in this calculation, the global level density is midway between a semicircle and a Gaussian distribution.

II. A RANDOM-MATRIX MODEL FOR NONERGODIC DISORDERED ENSEMBLES

To fix the ideas, let $H_G(\sigma)$ be a random matrix from GOE (with Dyson index $\beta = 1$) of dimension $N \times N$ with matrix elements chosen independently from the Gaussian distribution $\mathcal{N}(\mu, \sigma)$ with $\mathcal{N}(0, 1)$ for the diagonal elements, and $\mathcal{N}(0, 1/\sqrt{2})$ for the nondiagonal elements [22]. A new, so-called *disordered* random-matrix ensemble $H(\sigma, \xi)$ can be introduced by imposing an external source of randomness ξ to the fluctuations of the Gaussian matrix [15, 16],

$$H(\sigma, \xi) = \frac{H_G(\sigma)}{\sqrt{\xi/\bar{\xi}}}, \quad (1)$$

where ξ is a positive random variable chosen from a normalized probability distribution $w(\xi)$ with average μ_ξ and variance σ_ξ , and $\bar{\xi}$ is a constant that will control the intensity of the nonergodicity. It is possible to iteratively generate all the matrix elements of $H(\sigma, \xi)$: At the

ν th step, a new element is sorted through the relation,

$$h_\nu = \frac{h_G(\sigma)}{\sqrt{\xi_\nu/\bar{\xi}}}. \quad (2)$$

Here, h_G are the $f = N(N+1)/2$ independent Gaussian matrix elements, ordered in such a way that the first N ones are the diagonal elements H_{ii} , and the remaining ones are the rescaled off-diagonal elements $\sqrt{2}H_{ij}$. The reason for the factor $\sqrt{2}$ is explained in Ref. [17]. Subsequent values for the disorder random variable ξ_ν are sorted recursively from a disorder distribution,

$$w_\nu(\xi) = \frac{w_0(\xi)\xi^{(n-1)/2} \exp\left(-\frac{\beta\xi}{2\sigma^2\xi} \sum_{i=1}^{\nu-1} h_i^2\right)}{\int d\xi w_0(\xi)\xi^{(n-1)/2} \exp\left(-\frac{\beta\xi}{2\sigma^2\xi} \sum_{i=1}^{\nu-1} h_i^2\right)}. \quad (3)$$

Fixing the set of disorder variables $\xi_1, \xi_2, \dots, \xi_f$ during the realization of a particular matrix for the ensemble maintains the univariance of $w_\nu(\xi)$ at all time, and allows it to converge rapidly with iteration number ν to a very narrow and peaked distribution around a mean value μ_ξ , where the position of μ_ξ depends on the shape of the initial distribution $w_0(\xi)$. Consider now as a particular

choice for the distribution $w_0(\xi)$ the normalized gamma distribution,

$$w_0(\xi) = \exp(-\xi)\xi^{\bar{\xi}-1}/\Gamma(\bar{\xi}), \quad (4)$$

with $\mu_\xi = \bar{\xi}$ and $\sigma_\xi^2 = \bar{\xi}$. The mean $\bar{\xi}$ controls the behaviour of the distribution $w_0(\xi)$, which can be Gaussian-like (for $\bar{\xi} \ll 1$), or long-tailed (for $\bar{\xi} \gg 1$). The disorder distribution $w_\nu(\xi)$ will tend to converge to similar positions for Gaussian-like $w_0(\xi)$, and to different positions for long-tailed $w_0(\xi)$, see Fig. 1 (upper left insets). This can be understood through the coefficient of variation (CV) which considers standard deviation relative to the mean [23], which in the present case behaves as $CV = \sigma_\xi/\mu_\xi = 1/\sqrt{\bar{\xi}}$ and tends to zero for large $\bar{\xi}$. This means that for $\bar{\xi} \gg 1$ there will be little variation between the random initial positions for the disorder distribution, whereas for $\bar{\xi} \ll 1$ all initial positions will likely be very different. Finally, the factor $(\xi/\bar{\xi})^{-1/2}$ multiplying the Gaussian matrices in Eq. (1) acts on the variance σ^2 of the Gaussian ensembles. Subsequent realizations of the matrix are generated using different sets of ξ , and the variance of each matrix depends on the width of $w_0(\xi)$, which in this way defines the ergodicity of the ensemble. This can be appreciated in Fig. 1 (lower right insets), where the level density $\rho(E)$ is very similar for all realizations for $\bar{\xi} = 200$, but dissimilar for different realizations for $\bar{\xi} = 0.5$. Likewise, level sequences $E(n)$ evolve in similar ways for $\bar{\xi} = 200$, but behave differently for $\bar{\xi} = 0.5$ (main panel).

III. DATA-ADAPTIVE UNFOLDING USING SINGULAR VALUE DECOMPOSITION (SVD)

A. Trend and fluctuation normal modes

In the following, we briefly review the data-adaptive unfolding method of Ref. [21]. Consider an ensemble of $m = 1 \dots M$ level sequences $E^{(m)}(n)$, where each sequence consists of $n = 1 \dots N$ levels, such as the ensembles with $N = M = 50$ presented in Fig. 1 (main panel). Each sequence constitutes one of the rows of a $M \times N$ dimensional matrix \mathbf{X} , which we will interpret as a multivariate time series,

$$\mathbf{X} = \begin{pmatrix} E^{(1)}(1) & E^{(1)}(2) & \dots & E^{(1)}(N) \\ E^{(2)}(1) & E^{(2)}(2) & \dots & E^{(2)}(N) \\ \vdots & \vdots & \ddots & \vdots \\ E^{(M)}(1) & E^{(M)}(2) & \dots & E^{(M)}(N) \end{pmatrix}. \quad (5)$$

Singular Value Decomposition (SVD) is an exact and parameter-free matrix decomposition technique that allows us to rewrite \mathbf{X} in a unique way as,

$$\mathbf{X} = \mathbf{U}\mathbf{\Sigma}\mathbf{V}^T = \sum_{k=1}^r \sigma_k \vec{u}_k \vec{v}_k^T, \quad (6)$$

where $\mathbf{\Sigma}$ is an $M \times N$ -dimensional matrix with only diagonal elements that are the ordered *singular values* $\sigma_1 \geq \sigma_2 \geq \dots \geq \sigma_r$, where $r \leq \text{Min}[M, N] = \text{rank}(\mathbf{X})$. The vectors \vec{u}_k are orthonormal and they constitute the k th columns of the $M \times M$ -dimensional matrix \mathbf{U} . They are called the *left-singular vectors* of \mathbf{X} , and they span its column space. Their physical significance will be explained further on. The vectors \vec{v}_k are orthonormal and they constitute the k th columns of the $N \times N$ -dimensional matrix \mathbf{V} . They are called the *right-singular vectors* of \mathbf{X} , they span its row space, and therefore they constitute a basis of energy *normal modes* for the ensemble. The expression $\vec{u}_k \vec{v}_k^T \equiv \vec{u}_k \otimes \vec{v}_k$ indicates the outer product of \vec{u}_k and \vec{v}_k . A set $\{\sigma_k, \vec{u}_k, \vec{v}_k\}$ is called an *eigen triplet*, and completely defines the eigenmode of order k . Any matrix row of \mathbf{X} containing a particular eigenspectrum can be written as,

$$E^{(m)}(n) = \bar{E}(n) + \tilde{E}(n) = \sum_{k=1}^r \sigma_k U_{mk} \vec{v}_k^T(n), \quad (7)$$

where $\lambda_k = \sigma_k^2$ can be interpreted as *partial variances* that indicate how much a specific normal mode \vec{v}_k contributes to the total variance of the ensemble, and the matrix elements U_{mk} serve as coefficients that express a particular level sequence exactly as a weighted sum of normal modes. The normal modes \vec{v}_k with $k = 1, \dots, n_T$ that determine the global spectral properties \bar{E} of a particular spectrum behave monotonously and can easily be distinguished by their large partial variances λ_k that are orders of magnitude larger than the remaining λ_k with $k = n_T + 1, \dots, r$ associated to the oscillating normal modes of the fluctuations \tilde{E} [21]. In the present calculation, we find one global mode ($n_T = 1$) for the matrix ensembles in the ergodic regime, and two global modes ($n_T = 2$) in the nonergodic regime. In Fig. 1 (main panels), the data-adaptive global behaviour \bar{E} is shown for a particular level sequence, in comparison with the ensemble mean $\langle E \rangle$. The adaptive global level density is easily calculated as the histogram $\rho(\bar{E})$ of the data-adaptive global behaviour \bar{E} and is compared with the ensemble average $\langle \rho \rangle$ (lower right insets). It can be appreciated that in the ergodic regime the ensemble average $\langle E \rangle$ or $\langle \rho \rangle$ is representative for an individual spectral average \bar{E} or $\rho(\bar{E})$, whereas in the nonergodic regime the ensemble mean is not representative.

B. Fluctuation measures

In Ref. [21], we applied the above data-adaptive unfolding to ergodic Gaussian ensembles. On the one hand, the fluctuation part $k = n_T + 1, \dots, r$ of the *scree diagram* of ordered partial variances behaves as a power law,

$$\lambda_k \propto 1/k^\gamma, \quad (8)$$

which gives the *ensemble estimate* of the spectral rigidity in terms of how the normal modes \vec{v}_k common to all

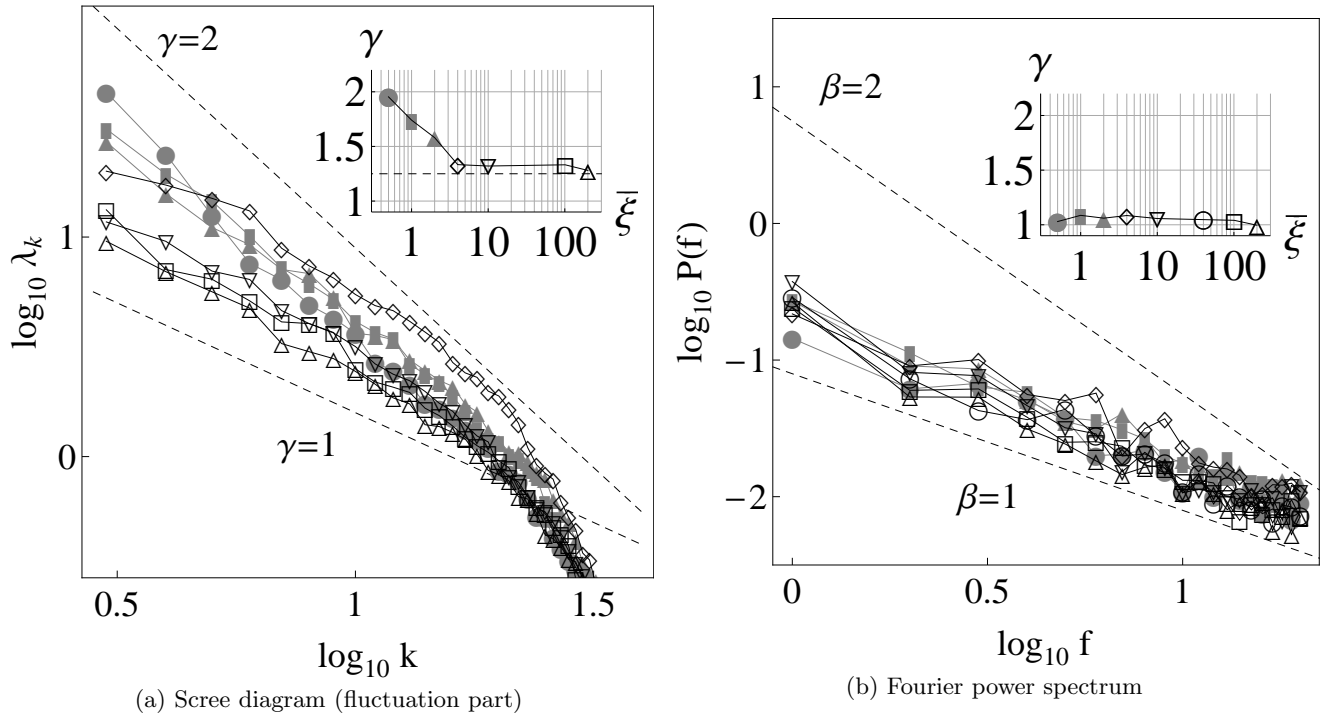


FIG. 2: Data-adaptive unfolding of eigenspectra in the nonergodic regime for $\bar{\xi} = 0.5, 1, 2$ (grey filled symbols) and in the ergodic regime $\bar{\xi} = 4, 10, 100, 200$ (black open symbols). (a) Ensemble perspective: The fluctuation part of the scree diagram λ_k changes its scaling behaviour from $\gamma = 2$ (Poisson statistics) for $\bar{\xi} = 0.5$ towards $\gamma < 1.5$ for $\bar{\xi} \geq 4$, compared with the numerical result $\gamma \approx 1.25$ for a very small GOE ensemble with $N = M = 50$ (horizontal dashed line). (b) Individual spectrum perspective: The Fourier power spectrum $P(f)$ of the fluctuations $\tilde{E} = E - \bar{E}$ of individual spectra results in $\beta = 1$ (GOE statistics) independently from $\bar{\xi}$.

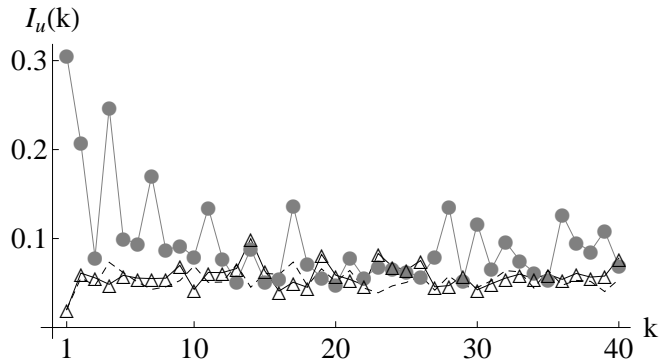


FIG. 3: Inverse Participation Ratio $I_u(k)$ of the left-singular vectors \tilde{u}_k . In the ergodic regime ($\bar{\xi} = 200$, black open triangles), $I_u(k)$ is low for most \tilde{u}_k indicating that these vectors are influenced by most spectra and thus are representative for the whole ensemble. In the nonergodic regime ($\bar{\xi} = 0.5$, gray filled circles), peaks of high $I_u(k)$ indicate that these vectors are influenced by one or only few spectra and thus are not representative for the whole ensemble. In comparison, results for $I_u(k)$ are shown for an ensemble of GOE spectra of the same dimensions $N = M = 50$ (black dashed lines).

eigenspectra scale. On the other hand, the Fourier power

spectrum of the fluctuations $\tilde{E}(n)$ of the individual spectra also follows a power law,

$$P(f) \propto 1/f^\beta. \quad (9)$$

which is the *spectrum estimate* of the spectral rigidity. For ergodic ensembles, it resulted that the spectral exponents of both estimates are equal [21]. The value $\beta = \gamma = 1$ characterizes correlated spectra of the GOE type because of level repulsion. The value $\beta = \gamma = 2$ reflects the Poissonian statistics of noncorrelated levels in the absence of level repulsion.

In the following, we apply the data-adaptive unfolding to eigenspectra of the disordered matrix ensemble of Sect. II. In Fig. 2 (panel (a)), the fluctuation part of the scree diagram λ_k is shown for different values of $\bar{\xi}$. Apart from a tail of nonsignificant λ_k for high-order modes when the basis becomes overcomplete, the power-law behaviour of Eq. (8) is observed for all realizations, and the value of the spectral exponent γ changes in function of $\bar{\xi}$ (see inset). For $\bar{\xi} = 0.5$, in the nonergodic regime, we find $\gamma = 2$ corresponding to Poisson statistics. The spectral exponent γ drops quickly for increasing $\bar{\xi}$, reflecting a rapid decrease of intensity of nonergodicity, as will be explained in the next subsection. For $\bar{\xi} \geq 4$, there is a further low approach to the ergodic limit,

in correspondence with the results of Ref. [15] for the fluctuation measure Σ_2 , obtained after a traditional ensemble unfolding. The expected value of $\gamma = 1$ for the ergodic limit is never obtained because of the small ensemble dimensions used in the present calculations $N = M = 50$, where the power law can be followed only over a very limited range of less than one order of magnitude. For a GOE ensemble with the same limited dimensions N and M , the numerical result $\gamma \approx 1.25$ is obtained.

On the other hand, in Fig. 2 (panel (b)), the Fourier power spectrum of the fluctuations \bar{E} of individual eigen-spectra follows the power law of Eq. (9) with spectral exponent $\beta = 1$, indicating GOE statistics, as indeed expected if the unfolding is carried out appropriately [15]. Moreover, the value for spectral exponent β is independent from $\bar{\xi}$. The spectral exponent γ approaches the value for β for larger values of the control parameter $\bar{\xi}$ when the ergodic limit is approached. The difference between the spectral exponents β and γ can serve as a measure of nonergodicity.

C. Inverse participation ratio and breakdown of the normal-mode basis

Now, we want to understand the value of the spectral exponent γ . The component m of a given left-singular vector \vec{u}_k relates to the contribution of spectrum m to that vector. Hence, the distribution of the components contains information about the number of spectra contributing to a specific left-singular vector. In order to distinguish between one vector with approximately equal components and another with a small number of large components, one can define the inverse participation ratio for a vector \vec{u}_k [25, 26],

$$I_u(k) \equiv \sum_{m=1}^M [\vec{u}_k(m)]^4. \quad (10)$$

The physical meaning of $I_u(k)$ can be illustrated by two limiting cases, (i) an eigenvector with identical components $\vec{u}_k(m) = 1/\sqrt{M}$ has $I_u(k) = 1/M$, whereas (ii) an eigenvector with one component $\vec{u}_k(m) = 1$ and all the others zero has $I_u(k) = 1$. Therefore, $I_u(k)$ is related to the reciprocal of the number of eigenvector components significantly different from zero.

In Fig. 3, we can see that in the nonergodic regime for $\bar{\xi} = 0.5$ almost half of the vectors \vec{u}_k has a very high inverse participation ratio $I_u(k)$, indicating that one or only few spectra contribute to the eigentriplet $\{\sigma_k, \vec{u}_k, \vec{v}_k\}$, so that this eigenmode is not representative for the whole ensemble. The scree diagram is thus composed of many noncorrelated partial variances, resulting in Poissonian statistics. In the ergodic regime, for $\bar{\xi} = 200$, inverse participation ratios $I_u(k)$ are small,

indicating that most if not all spectra contribute to the eigentriplets, which are thus representative for the whole ensemble. The scree diagram is composed of fully correlated partial variances and results in GOE statistics. The few moderate peaks that appear in $I_u(k)$ for $\bar{\xi} = 200$ with respect to the results for a GOE ensemble of the same dimensions $N = M = 50$ indicates that the fully ergodic limit has not yet been reached.

In this context, nonergodicity can be understood as a breakdown of the common normal-mode basis of the ensemble, not only at the large energy scale of the global spectral behaviour \bar{E} , see Fig. 1 (main panels), but also at the small scale of the local fluctuations \bar{E} , see Fig. 2 (panel (a)). The inverse participation ratio $I_u(k)$ can serve as a measure for nonergodicity.

D. Rescaling

With the present data-adaptive unfolding applied here the spectra are not rescaled but only detrended. This is a disadvantage if the purpose is to calculate traditional fluctuation measures such as the short-range nearest-neighbour spacing distribution or the long-range Σ_2 or Δ_3 measures, which require an explicit normalization of the fluctuations [1]. Time-series based fluctuation measures such as the scree diagram λ_k or the Fourier power spectrum $P(f)$ absorb the scale of the fluctuations in the offset of the power law of Eqs. (8) and (9), whereas the statistics of the fluctuations is codified in the spectral exponents γ and β .

This can be illustrated with Fig. 2 (panel (a)), where the offset of the fluctuation part of the scree diagram varies over almost a whole order of magnitude. For $\bar{\xi} \gg 1$, the factor that determines the variance of the ensemble $(\xi/\bar{\xi})^{-1/2} \rightarrow 1$, and the variance of the disordered ensemble $H(\sigma, \xi)$ tends to remain unchanged with respect to the initial Gaussian ensemble $H(\sigma)$ (curves with black open symbols). For $\bar{\xi} \ll 1$, the factor $(\xi/\bar{\xi})^{-1/2}$ can become very large because of the divergence of $w_0(\xi)$ near $\xi = 0$, and the variance of the disordered ensemble is enhanced (curves with grey filled symbols). The case $\bar{\xi} = 4$ is intermediate between these two regimes.

IV. CONCLUSIONS

In the present contribution, we applied a data-adaptive unfolding technique that we initially presented for canonical Gaussian ensembles to a disordered random-matrix model, which allows to finetune the intensity of nonergodicity. We calculated ensemble-averaged and spectrum-averaged statistics in a parameter-free and consistent way within the same data-adaptive basis of normal modes. In this context, nonergodicity can be explained as the

breakdown of the common normal-mode basis. The inverse participation ratio, and the difference between the spectrum-averaged and the ensemble-averaged statistics can serve as measures for the intensity of nonergodicity.

Acknowledgements

The author acknowledges financial support from CONACYT (Grants No. CB-2011-01-167441 and No.

CB-2010-01-155663). This work was also partly funded by the Instituto Nacional de Geriatria (project DI-PI-002/2012). The author wishes to thank G. Torres Vargas, J. C. López Vieyra and V. Velázquez for fruitful discussions, and wishes to thank also the anonymous referee of our previous publication who brought the interesting topic of nonergodicity to our attention.

-
- [1] M. L. Mehta, *Random matrices* (Acad. Press, New York, 1991), 2nd ed.
- [2] F. Haake, *Quantum signatures of chaos* (Springer, Heidelberg, 2010), 3rd ed.
- [3] J. Kwapień and S. Drożdż, *Phys. Rep.* **515**, 115 (2012).
- [4] L. Benet, T. Rupp and H. A. Weidenmüller, *Phys. Rev. Lett.* **87**, 010601 (2001).
- [5] T. Asaga, L. Benet, T. Rupp and H. A. Weidenmüller, *Europhys. Lett.* **56**, 340 (2001).
- [6] A. D. Jackson, C. Mejia-Monasterio, T. Rupp, M. Saltzer and T. Wilke, *Nucl. Phys. A* **687**, 405 (2001).
- [7] C. Male, G. Le Caër and R. Delannay, *Phys. Rev. E* **76**, 042101 (2007).
- [8] A. Relaño, L. Muñoz, J. Retamosa, E. Faleiro and R. A. Molina, *Phys. Rev. E* **77**, 031103 (2008).
- [9] J. B. French and S. S. M. Wong, *Phys. Lett. B* **33**, 449 (1970); O. Bohigas and J. Flores, *ibid.* **34**, 261 (1971); J. B. French and S. S. M. Wong, *ibid.* **35**, 383 (1971).
- [10] J. Flores, M. Horoi, M. Müller and T. H. Seligman, *Phys. Rev. E* **63**, 026204 (2001).
- [11] K. K. Mon and J. B. French, *Ann. Phys.* **95**, 90 (1975); L. Benet and H. A. Weidenmüller, *J. Phys. A: Math. Gen.* **36**, 3569 (2003).
- [12] P. Cizeau and J. P. Bouchaud, *Phys. Rev. E* **50**, 1810 (1994).
- [13] T. Guhr and H. A. Weidenmüller, *Ann. Phys. (N.Y.)* **199**, 412 (1990); M. S. Hussein and M. P. Pato, *Phys. Rev. Lett.* **70**, 1089 (1993).
- [14] G. Biroli, J. P. Bouchaud and M. Potters, *Acta Phys. Pol. B* **38**, 4009 (2007).
- [15] O. Bohigas, J. X. de Carvalho and M. P. Pato, *Phys. Rev. E* **77**, 011122 (2008).
- [16] O. Bohigas and M. P. Pato, *Phys. Rev. E*, 031121 (2011).
- [17] F. Toscano, R. O. Vallejos and C. Tsallis, *Phys. Rev. E* **69**, 066131 (2004).
- [18] A. C. Bertuola, O. Bohigas and M. P. Pato, *Phys. Rev. E* **70**, 065102(R) (2004).
- [19] J. M. G. Gómez, R. A. Molina, A. Relaño and J. Retamosa, *Phys. Rev. E* **66**, 036209 (2002).
- [20] S. M. Abuelenin and A. Y. Abul-Magd, *Pocedia CS* **12**, 69 (2012).
- [21] R. Fossion, G. Torres Vargas and J. C. López Vieyra, *Phys. Rev. E* **88**, 060902(R) (2013).
- [22] A. Edelman and N. Raj Rao, *Acta Num.* **14**, 233 (2005).
- [23] R. Fossion, D. A. Hartasánchez, O. Resendis-Antonio and A. Frank, *Front. Biol.* **8**, 247 (2013).
- [24] A. Relaño, J. M. G. Gómez, R. A. Molina, J. Retamosa and E. Faleiro, *Phys. Rev. Lett.* **89**, 244102 (2002).
- [25] V. Plerou, P. Gopikrishnan, L.A. Nunes Amaral and H. Eugene Stanley, *Phys. Rev. Lett.* **83**, 1471 (1999).
- [26] V. Plerou, P. Gopikrishnan, B. Rosenow, L.A. Nunes Amaral, T. Guhr and H. Eugene Stanley, *Phys. Rev. E* **65**, 066126 (2002).